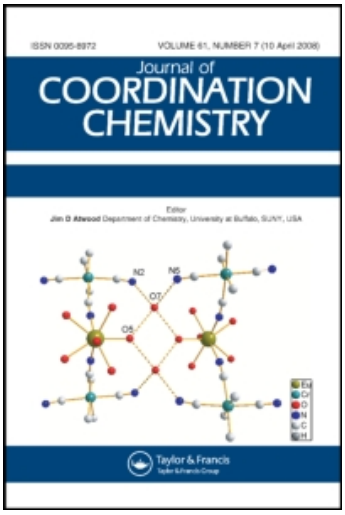

Journal of Coordination Chemistry
Publication details, including instructions for authors and subscription information:
http://www.informaworld.com/smpp/title~content=t713455674

STRUCTURAL STUDIES ON PYRAZOLYLPYRIDINE LIGANDS AND COMPLEXES. COMPARISONS BETWEEN LINKAGE ISOMERS AND WITH 2,2'-BIPYRIDINE

Yue Luo[a]; Pierre G. Potvin[a]
[a] Department of Chemistry, York University, North York, Ontario, Canada

To cite this Article Luo, Yue and Potvin, Pierre G.(1999) 'STRUCTURAL STUDIES ON PYRAZOLYLPYRIDINE LIGANDS AND COMPLEXES. COMPARISONS BETWEEN LINKAGE ISOMERS AND WITH 2,2'-BIPYRIDINE', Journal of Coordination Chemistry, 46: 3, 319 — 334
To link to this Article: DOI: 10.1080/00958979908048477
URL: http://dx.doi.org/10.1080/00958979908048477

J. Coord. Chem., 1999, Vol. 46, pp. 319–334
Reprints available directly from the publisher
Photocopying permitted by license only

STRUCTURAL STUDIES ON PYRAZOLYLPYRIDINE LIGANDS AND COMPLEXES. COMPARISONS BETWEEN LINKAGE ISOMERS AND WITH 2,2′-BIPYRIDINE

YUE LUO and PIERRE G. POTVIN*

Department of Chemistry, York University, 4700 Keele Street, North York, Ontario, Canada M3J 1P3

(Received 27 May 1997; Revised 1 October 1997; In final form 24 March 1998)

Crystal structures were obtained for the 3′(*C*),2-linked pyrazolylpyridines 2*H*-3-(pyridin-2-yl)-4,5,6,7-tetrahydroindazole (**1**) and 1-(4″-ethoxycarbonylphenyl)-3-(pyridin-2-yl)-4,5,6,7-tetrahydroindazole (**2**), and for the Zn^{II} complex of the methyl ester analog of **2**, ($Zn(\mathbf{3})Cl_2$). With **2** found in the *anti* rotameric conformation, ligand distortion was assessed in the *syn* forms found in **1** (treated as a H^+ complex), $Zn(\mathbf{3})Cl_2$ and $[Ru(bpy)(\mathbf{2})_2](PF_6)_2$. Several differences were noted from similar analyses on structures for representative Zn^{II} and Ru^{II} complexes of bipyridine or 1,10-phenanthroline, for complexes of other 3′(*C*),2-linked 2-(pyrazol-3-yl) pyridines and for complexes of isomeric 1′(*N*′),2-linked 2-(pyrazol-l-yl)pyridines. A notable finding is that bpy and the *N*′,2-linked pyrazolylpyridines lose planarity upon complex formation due to steric congestion between the rings, whereas **1** and complexed **2** or **3** remain coplanar, a difference attributable to differences in the bond lengths and angles at the binding locus. Comparisons between pyrazolylpyridine linkage isomers additionally revealed that the metal binding is at more ideal angles with the *C*-linked ligands and the bond length distortions occur mostly within the pyrazole ring, whereas the pyridine ring suffers more in the *N*-linked ligands.

Keywords: Pyrazolylpyridine complexes; bipyridine complexes; crystal structures; ligand distortions; transition metal binding

* Corresponding author. Tel.: (416) 736-2100. Ext. 66140. Fax: (416) 736-5936.
E-mail: pgpotvin@yorku.ca.

INTRODUCTION

The utility of 2,2′-bipyridine (bpy) in coordination chemistry has spurred the exploration of other α,α'-diimino bidentate ligands built from combinations of azoles and azines,[1] including the relatively π-rich pyrazolylpyridines. In previous reports, we presented a series of bidentate,[2] tridentate,[3] pentadentate[4] and macrocyclic[4] ligands based on the novel 3′(*C*′),2-linked 2-(tetrahydroindazol-3-yl)pyridine, of which **1** is the simplest example. These are available in short, high-yielding routes from readily available materials. They constitute linkage isomers of 1′(*N*′),2-linked 2-(pyrazol-1-yl)pyridines.[5,6]

Though there have been until recently no crystal structures of free pyrazolylpyridine ligands[7] and only a few of their complexes,[8–14] the two linkage isomers and bpy are expected to present significantly different geometries at the central α,α'-diimine binding site and these will affect the complexes. In the present work, we report the crystal structures of metal-free *C*′,2-linked pyrazolylpyridines **1** and **2**, and of a Zn^{II} complex. Along with data from the previously reported Ru^{II} complex and literature data involving other bidentate ligands, these structures allow a comparative assessment of the ligands' binding locus and the changes incurred upon complexation. Some differences in solution-state properties are also discussed.

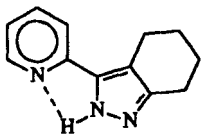

1

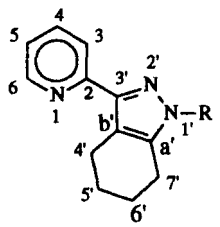

2 R = C_6H_4-4"-$COOCH_2CH_3$
3 R = C_6H_4-4"-$COOCH_3$
4 R = CH_3

EXPERIMENTAL

The preparations of **1**, **2** and Zn(**3**)Cl_2 have been detailed elsewhere.[2] Suitable crystals of **1** and **2** were obtained from EtOAc at room temperature. Crystals of Zn(**3**)Cl_2 were grown from MeOH over 4 days. All were colorless. Reflection data were collected on a Siemens R3m/V diffractometer equipped with graphite-monochromatized MoKα radiation ($\lambda = 0.71073$ Å)

at 295 K, using a $\omega/2\theta$ scan. Intensity data were corrected for Lorentz and polarization effects but not for absorption. The structures were solved by the direct method, using the Siemens SHELXTL PLUS software, then with SHELXL-93,[35] with which all non-hydrogen atoms were refined on F^2 anisotropically by full-matrix least-squares, to a maximum $\Delta/\sigma < 0.001$. Hydrogen atoms were included at idealized positions using a riding model, including pairs at C(3) and C(6) for each conformer of **2**, with isotropic thermal parameters of 0.08 Å^2. The refinement statistic and weighting schemes were $wR(F^2) = [\Sigma w(F_o^2 - F_c^2)^2/\Sigma wF_o^4]^{1/2}$, where $w^{-1} = \sigma^2(F_o^2) + (aP)^2 + bP$, with $3P = (max\{F_o^2,0\} + 2F_c^2)$ and a and b are constants internally adjusted according to the analysis of variance. The conventional statistic $R(F) = \sum||F_o|-|F_c||/\sum|F_o|$ is quoted for comparison.

Crystal Structure Determination of 1

Crystal Data

$C_{12}H_{13}N_3$, $M = 199.25$, orthorhombic, $a = 6.864(2)$, $b = 17.122(5)$, $c = 17.853(4)$ Å, $U = 2098.2(10)$ Å^3, space group *Pbca*, $Z = 8$, $D_c = 1.262$ Mg m^{-3}, $F(000) = 848$, crystal dimensions $0.8 \times 0.3 \times 0.05$ mm, $\mu = 0.078$ mm^{-1}, data collection range $2.28 < \theta < 25.00°$, index ranges $-1 \leq h \leq 7$, $-1 \leq k \leq 20$, $-1 \leq l \leq 21$, 2351 reflections collected, 1753 unique ($R_{int} = 0.1164$), which were used in all calculations.

Structure Refinement

The *N*-H in **1** was located with a Fourier difference contour map constructed using the Siemens software from a refinement model lacking that hydrogen. Refinement of its coordinates and isotropic displacement parameter led to a pyramidalized N and a short N–H distance. Refinement of only the N–H distance along the idealized bond vector also led to a short bond length. Neither model made a significant impact on the refinement statistics. The final $wR(F^2)$ was 0.2084 for 136 parameters, corresponding to $R(F) = 0.0898$ for 559 data where $F_o > 4\sigma(F_o)$, g.o.f. 1.031, maximum $\Delta\rho = 0.186$ e Å^{-3} in the vicinity of C(9).

Crystal Structure Determination of 2

Crystal Data

$C_{21}H_{21}N_3O_2$, $M = 347.41$, monoclinic, $a = 10.982(2)$, $b = 7.970(2)$, $c = 20.329(4)$ Å, $\beta = 94.98(3)°$, $U = 1772.6(7)$ Å^3, space group $P2_1/c$, $Z = 4$,

$D_c = 1.302\,Mg\,m^{-3}$, $F(000) = 736$, crystal dimensions $0.8 \times 0.5 \times 0.3$ mm, $\mu = 0.085\,mm^{-1}$, data collection range $1.86 < \theta < 25.00°$, index ranges $-1 \leq h \leq 11$, $-1 \leq k \leq 9$, $-24 \leq l \leq 24$, 4065 reflections collected, 3011 unique ($R_{int} = 0.0242$), which were used in all calculations.

Structure Refinement

The final $wR(F^2)$ was 0.1398 for 255 parameters, including an extinction coefficient of 0.013(2), corresponding to $R(F) = 0.0462$ for 2100 data where $F_o > 4\sigma(F_o)$, g.o.f. 1.022, maximum $\Delta\rho = 0.182\,e\,Å^{-3}$ in the vicinity of C(20).

Crystal Structure Determination of $Zn(3)Cl_2$

Crystal Data

$C_{20}H_{19}Cl_2N_3O_2Zn$, $M = 469.65$, monoclinic, $a = 14.983(3)$, $b = 8.7250(10)$, $c = 17.055(2)$ Å, $\beta = 111.92°$, $U = 2068.4(5)$ Å^3, space group $P2_1/c$, $Z = 4$, $D_c = 1.508\,Mg\,m^{-3}$, $F(000) = 960$, crystal dimensions $0.4 \times 0.3 \times 0.1$ mm, $\mu = 1.466\,mm^{-1}$, data collection range $2.44 < \theta < 25.00°$, index ranges $-1 \leq h \leq 17$, $-1 \leq k \leq 10$, $-20 \leq l \leq 19$, 4682 reflections collected, 3648 unique ($R_{int} = 0.0410$), which were used in all calculations.

Structure Refinement

The final $wR(F^2)$ was 0.1204 for 253 parameters, corresponding to $R(F) = 0.0478$ for 2603 data where $F_o > 4\sigma(F_o)$, g.o.f. 1.054, maximum $\Delta\rho = 0.612\,e\,Å^{-3}$ in the vicinity of the metal.

Molecular Modeling

The structures of the *anti* forms of **4** (114 electrons, 31 *s* shells, 16 *sp* shells, 95 basis functions, final $E(HF) = -656.2520037$ a.u.), **6** (92 electrons, 24 *s* shells, 13 *sp* shells, 76 basis functions, final $E(HF) = -541.6647472$ a.u.) and **7** (118 electrons, 30 *s* shells, 17 *sp* shells, 98 basis functions, final $E(HF) = -692.4594953$ a.u.) were calculated under the RHF/STO-3G model with geometry optimization (to $< 10^{-7}$ a.u.), using the *Spartan v3.1.2* suite of programs (Wavefunction Inc., 18401 Von Karman, Suite 370, Irvine CA 92715) on a Silicon Graphics Indigo R4000 workstation. Molecular symmetry was not enabled and all molecules were neutral with multiplicity 1. The structure of *syn*-**4** (final $E(HF) = -656.2502436$ a.u.) was obtained while constraining to 0° the appropriate dihedral angles.

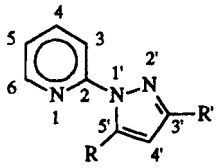

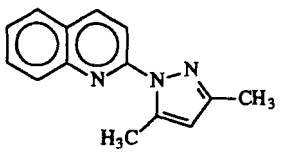

7

5 R = R' = H
6 R = R' = CH_3
8 R = H, R' = C_5H_4FeCp
9 R = H, R' = C_6H_3-2",5"-$(OCH_3)_2$

Distortion Analysis

The atomic positional parameters from structures cited for comparison with those reported herein were obtained either directly from the literature reports or from databases according to instructions given by the authors. They were converted to Cartesian coordinates to calculate bond lengths, bond angles, bite angles, idealized binding distances and least-squares planes for non-hydrogen atoms. All calculations ignored the uncertainties in atomic positions. The calculation of the least-squares planes and the average bond length changes upon complexation reported herein neglected the C5–C6 bridge in phen, the benzo ring in 7 and all other ring substituents.

Inter-ring angles were calculated as the angles between the normals of the least-squares planes defined by the non-hydrogen atoms in each ring. Interplanar dihedral (twist) angles were measured while viewing these normals along the centroid-to-centroid axis. Ligand bowing was measured as the inter-ring angle remaining after correction by rotation about the inter-ring bond of any inter-ring dihedral to 0°. The distance between imino nitrogens was assessed after a similar correction to flat, *syn* rotamers.

RESULTS

3-(Pyridin-2-yl)-4,5,6,7-tetrahydroindazole, the *C'*,2-linked pyrazolylpyridine **1**, can exist in two tautomeric forms (1*H* vs. 2*H*), each of which may adopt one of two rotational conformations about the pyridine–pyrazole bond (with *syn* and *anti* nitrogens). Further, the fused cyclohexane ring can adopt one of two half-chair conformations. Though these interchange rapidly in solution, they can be enantiomeric in the solid state, if the rest of the molecule is flat, or diastereomeric, if not. X-ray diffraction by a single crystal of **1** shows that it adopts the *syn* conformer of the in^2 (or 2*H*) tautomer (Figure 1), the same as in solution.[2] The *in* position of the N-*H*

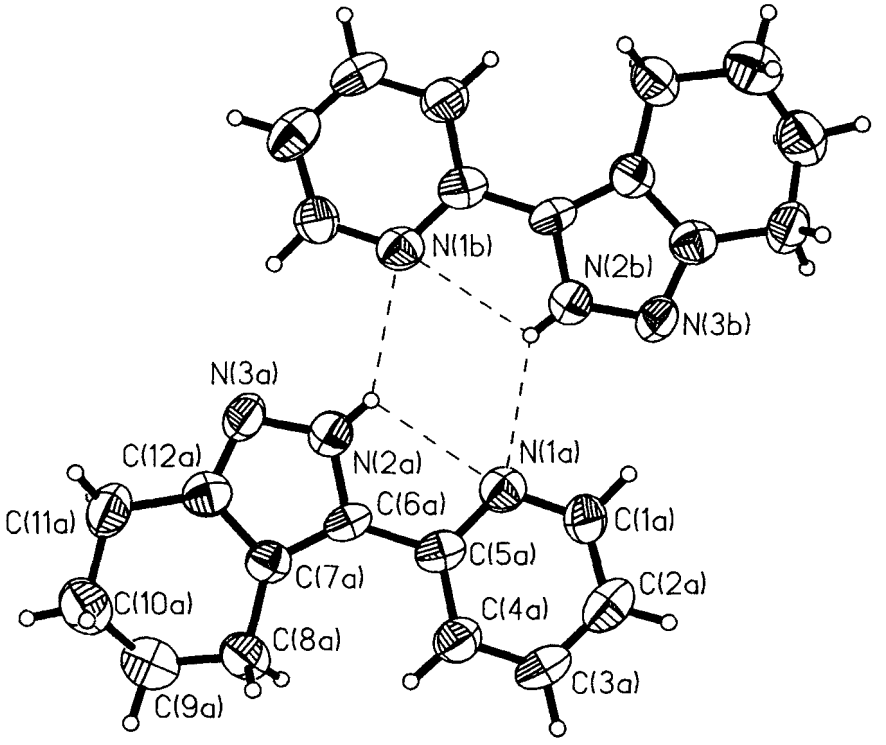

FIGURE 1 ORTEP view of a dimer pair of **1** (related by crystallographic symmetry) using 50% probability thermal ellipsoids. Selected bond lengths (in Å) and angles (in °): N(1)–C(1) 1.354(8), C(1)–C(2) 1.385(8), C(2)–C(3) 1.383(9), C(3)–C(4) 1.388(8), C(4)–C(5) 1.395(8), C(5)–N(1) 1.354(7), C(5)–C(6) 1.481(8), C(6)–N(2) 1.379(7), N(2)–N(3) 1.359(7), N(3)–C(12) 1.317(8), C(12)–C(7) 1.407(8), C(7)–C(6) 1.364(8), C(1)–N(1)–C(5) 116.2(6), N(1)–C(5)–C(6) 118.1(7), C(5)–C(6)–N(2) 118.7, C(6)–N(2)–N(3) 112.2, N(2)–N(3)–C(12) 104.4.

was ascertained from Fourier difference maps. All other hydrogens were linked to those of the attached carbons (riding model) at idealized positions. The pyrazole and pyridine rings are not quite coplanar, with an inter-ring dihedral angle of 1.7° and a bend of 2.5°. Molecules of **1** are packed in antiparallel stacks such that each forms a hydrogen-bonded dimer with a coplanar enantiomer on a neighboring stack. Figure 1 depicts such a dimer pair, showing both intra- and intermolecular H-bonding at N–H···N distances of 2.448 and 2.417 Å, respectively. We also noted a close intermolecular C6′–H···N1 contact (C(1)–H···N(3) in Figure 1) of 2.446 Å. However, the ^{1}H-NMR spectrum was constant over a 200-fold range of concentrations, implying the existence in solution of only monomeric units engaged in only intramolecular H-bonding.

The crystal structure of ethyl ester **2** is shown in Figure 2. It adopts the expected *anti* rotational conformation, as found for bpy[15] and tpy.[16] Persistent Fourier peaks in the middle of the tetramethylene bridge delineating the alternative half-chair conformation indicated conformational variation. When this was modelled as a disordered system with an 87:13 ratio of the two half-chairs, the refinement was significantly improved according to the Hamilton *R*-ratio test.[17] The molecule is not flat and these half-chairs are diastereomeric. Relative to the pyrazole ring, the pyridine ring is twisted 18.2° out of plane. The phenyl ring, which seems to be freely rotating in solution,[2] is similarly rotated 14.2° out of the pyrazole plane.

The crystal structure of the $ZnCl_2$ complex of the analogous methyl ester **3** (Figure 3) confirms the expected tetrahedral coordination to the metal. The Zn^{2+} binding is asymmetric, but both the longer Zn–N (pyridine) bond (2.083 Å) and the shorter Zn–N (pyrazole) bond (2.046 Å) are close in length to those of similar bonds in other crystals (2.088 Å average for bpy complexes[18–21] and 2.034 Å average in a tetrahedral trispyrazolylborate complex[22]). In these and other complexes of pyridylazoles,[9,10,23] the metal-to-azole bond is shorter than the metal-to-pyridine bond. The pyridine and

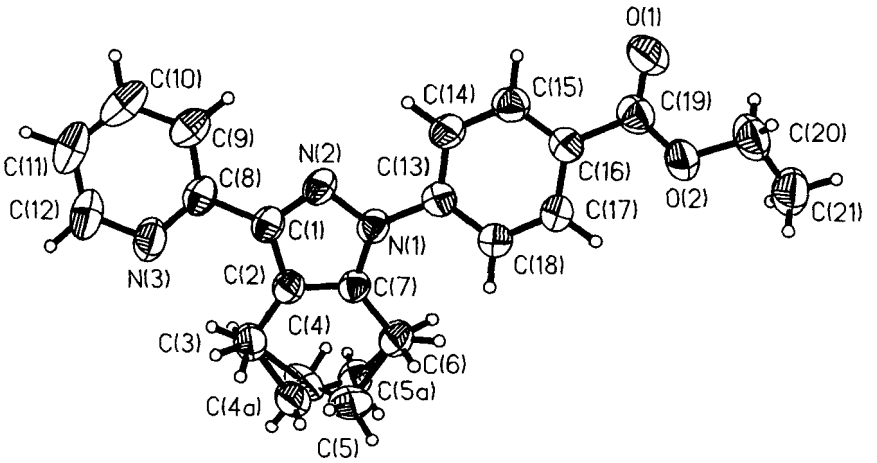

FIGURE 2 ORTEP plot of **2** with 50% probability thermal ellipsoids. Both conformers, C(3)–C(4)–C(5)–C(6) and C(3)–C(4a)–C(5a)–C(6), are shown and occur in 87:13 ratio, respectively. H atoms have been omitted for clarity. Selected bond lengths (in Å) and angles (in °): N(3)–C(12) 1.337(3), C(12)–C(11) 1.362(4), C(11)–C(10) 1.371(4), C(10)–C(9) 1.385(3), C(9)–C(8) 1.381(3), C(8)–N(3) 1.338(3), C(8)–C(1) 1.480(3), C(1)–N(2) 1.330(3), N(2)–N(1) 1.368(2), N(1)–C(7) 1.377(3), C(7)–C(2) 1.360(3), C(2)–C(1) 1.416(3), N(1)–C(13) 1.420(3), C(12)–N(3)–C(8) 117.3(2), N(3)–C(8)–C(1) 116.4(2), C(8)–C(1)–N(2) 119.6(2), C(1)–N(2)–N(1) 104.8(2), N(2)–N(1)–C(7) 111.1(2), N(2)–N(1)–C(13) 118.1(2).

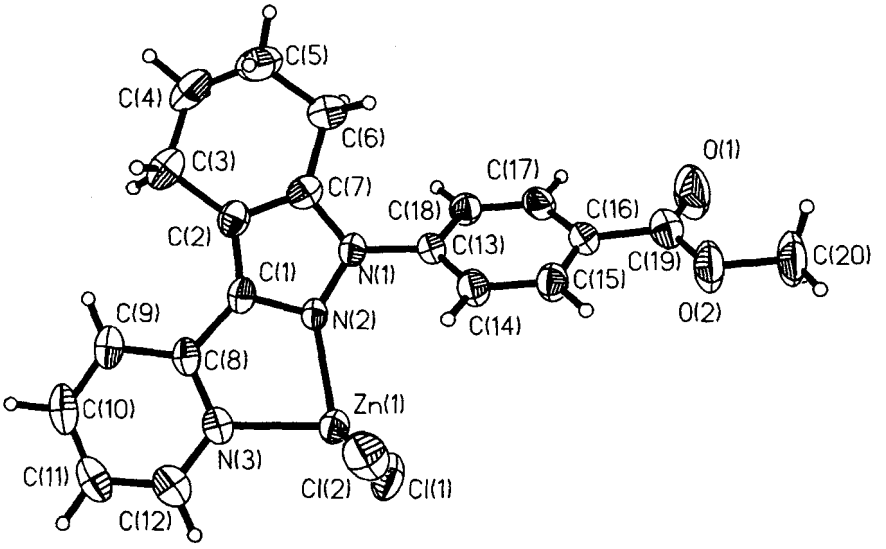

FIGURE 3 ORTEP view of $Zn(3)Cl_2$ using 50% probability thermal ellipsoids. Selected bond lengths (in Å) and angles (in °): Zn(1)–N(2) 2.046(3), Zn(1)–N(3) 2.082(3), Zn(1)–Cl(1) 2.1881(13), Zn(1)–Cl(2) 2.2118(14), N(3)–C(12) 1.345(5), C(12)–C(11) 1.379(6), C(11)–C(10) 1.369(7), C(10)–C(9) 1.370(7), C(9)–C(8) 1.381(5), C(8)–N(3) 1.351(5), C(8)–C(1) 1.477(6), C(1)–N(2) 1.353(5), N(2)–N(1) 1.359(4), N(1)–C(7) 1.356(5), C(7)–C(2) 1.370(6), C(2)–C(1) 1.392(6), N(1)–C(13) 1.428(5), Zn(1)–N(3)–C(8) 114.5, Zn(1)–N(2)–C(1) 115.1, N(2)-Zn(1)–N(3) 79.19(13), Cl(1)–Zn(1)–Cl(2) 121.93(6), C(12)–N(3)–C(8) 118.9(3), N(3)–C(8)–C(1) 114.7(3), C(8)–C(1)–N(2) 115.8(3), C(1)–N(2)–N(1) 105.2(3), N(2)–N(1)–C(7) 110.6(3), N(2)–N(1)–C(13) 121.3(3).

pyrazole rings are essentially coplanar but bent by 1.8°. The phenyl ring is twisted 50.2°, probably to avoid steric interactions with the $ZnCl_2$ portion.

$Zn(phen)Cl_2$[24] (phen is 1,10-phenanthroline) is the closest bipyridine analog to $Zn(\mathbf{3})Cl_2$. It is surprisingly asymmetric, exhibiting somewhat shorter Zn–N bond lengths (averaging 2.061 Å) than in bipyridine complexes, and with a 9.7° tilt of the $ZnCl_2$ plane from orthogonality to the binding plane (the mean square plane of the N–C–C–N binding locus). Moreover, the Zn atom sits 0.058 Å above the binding plane and the Cl–Zn–Cl angle is 114.7°. In $Zn(\mathbf{3})Cl_2$, the $ZnCl_2$ and N–C–C–N binding planes are more nearly orthogonal (88.2°) but the Zn lies 0.193 Å above the binding plane; in reflection of the weaker bite (Table I) the Cl–Zn–Cl angle is broadened to 121.9°.

The crystal structure of $[Ru(\mathbf{2})_2(bpy)](PF_6)_2$ (Figure 4) was briefly described earlier[25] and provides useful comparisons. Although it is C_2-symmetric in solution, it contains two distinct units of **2** (types I and II) and the bpy ligand is asymmetrically bound. The type II unit of **2** is the most asymmetrically bound, with the largest bond length and angle changes occurring

TABLE I Binding characteristics of bipyridines and pyrazolylpyridines

Ligand	*Bite angle* (°)	*Ideal M–N distances*/Å[a]	*N1–N2' span*/Å[b]
bpy[c]	64.4	2.526	2.691
phen[d]	61.6	2.702, 2.609	2.724
	62.4	2.632	2.725
1	57.5	2.924, 2.852	2.780
2	55.1	3.071, 2.818	2.732
8[e]	54.6	3.058, 2.746	2.677

[a]With pyrazolylpyridines, the longer distances are to pyridine N. [b]After rotation to the flat, *syn* form, if necessary. [c]Calculated from data in Ref. 15. [d]Calculated from data in Ref. 28. There are two distinct phen molecules in the crystal and one is asymmetric. [e]Calculated from data in Ref. 7.

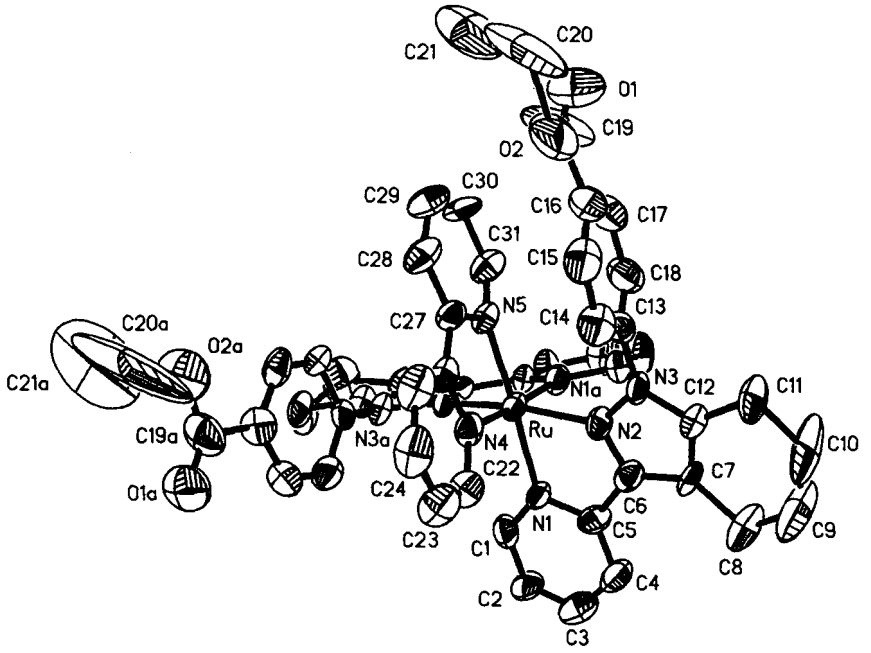

FIGURE 4 ORTEP view of $[Ru(bpy)(2)_2 1](PF_6)_2$ using 25% probability thermal ellipsoids with selected atoms labelled, from Ref. 25. H, P and F atoms have been omitted for clarity.

at the pyrazole ring. The four pyridine ring nitrogens form a nearly flat equatorial plane. The pyrazole rings lean back from the axial positions while their benzoate ester substituents point outward over either face of the bipyridine ligand. In order to do this, the phenyl rings are rotated into near orthogonality to the pyrazole rings (by 77.4 and 88.7°, respectively), much more than in the $ZnCl_2$ adduct. This amount of twisting out of conjugation effectively eliminates any resonance contribution of an aromatic substituent such as a phenyl group on the electronic properties of the pyrazolylpyridine

core, and fits our observation with a number of Ru^{II} complexes that the presence of this or other phenyl substituents exerted little effect on the oxidation potentials and the MLCT band positions.[25] In the present case, each phenyl ring hovers over its own pyridine ring of the bpy ligand at centroid-to-centroid distances of 3.56 and 3.64 Å, respectively, and forming phenyl-to-pyridine interplanar angles of 11.5° and 12.6°, respectively, thus allowing for strong $\pi-\pi$ stacking interactions. The bpy pyridine rings in turn tilt away, out of the equatorial plane (by 7.6° and 6.4°, respectively) forming a net interpyridine dihedral angle of 6.7°. In contrast, the pyrazole and pyridine rings in each of the units of **2** remain comparatively coplanar, as was the case in the Zn complex, with inter-ring dihedral angles of 0.3° and 2.3°, respectively.

DISCUSSION

Free Ligand Structures

According to NMR spectra in solution, the *anti* conformation in free *C'*,2-linked pyrazolylpyridines such as **2** can be distinguished from the *syn* conformation arising upon binding a metal (or H^+/D^+) because the latter places the pyridine H3 and the indazole C4′ hydrogens in sufficient proximity to partake in a mutual shielding interaction.[2–4] The *syn* form for **1** was similarly deduced. An alternative view of the process[26] invokes a relative deshielding of the pyridine H3 in the free, *anti* ligand by the pyrazole N2′ lone pair, the release of which indicates a change to the *syn* form. Our view is supported by the short distances between the appropriate pairs of hydrogens in the *syn* conformers in **1** and in $Zn(\mathbf{3})Cl_2$. The diastereotopic indazole hydrogens at C4′ are rendered equivalent in solution by rapid half-chair-to-half-chair transitions, and thus it is the averaged H···H distances that are relevant. These were 2.45 Å in $Zn(\mathbf{3})Cl_2$ and 2.34 Å in **1**, short enough for mutual shielding. In $[Ru(bpy)(\mathbf{2})_2](PF_6)_2$,[25] the average for both units of **2** was 2.61 Å. This through-space interaction was also directly observed by proximity-dependent NOE difference spectroscopy.[25,27]

Interestingly, an *in computo* rotation of the pyridine–pyrazole bond in free **2** from an *anti* to a *syn* conformation (with coplanarity as measured by an interplanar dihedral angle of 0°) produced a significantly shorter average H3···H4′ approach of 2.14 Å. This distance widened to 2.31 Å in the STO-3G-calculated structure of the *N*-methyl analog **4** in its *syn* conformation (constrained to be flat), suggesting that steric repulsions force these hydrogens apart. At the same time, the bite angle increased by 4° compared

to the *anti* form (see below). The widened distances in **1** therefore probably result largely from distortions due to such steric repulsions, with little more being contributed by the H-bonding, while those in $Zn(\mathbf{3})Cl_2$ and $[Ru(bpy)(\mathbf{2})_2](PF_6)_2$ are supplemented by complexation-induced distortions of the binding locus (see below).

By comparison, the closest H3···H3′ approach in bpy was similarly found to be even shorter, at 2.05 Å, but the closest H3′···H_3C approaches in the STO-3G structures of **6** and **7** were just 1.83 and 1.89 Å, respectively, highlighting the much stronger steric congestion in the undistorted *syn* forms of these compounds. This congestion is bound to cause severe distortion and this was evident during attempts to model the *syn* forms of **6** and **7**. With no constraints applied, the coplanar structures were unstable with respect to strongly twisted forms and, in attempts to counter this with strong dihedral constraints, severe out-of-plane ring distortions resulted.

Table I summarizes some binding-related structural differences between bipyridines and pyrazolylpyridines from crystal structures. The only crystal structure of an *N*′,2-linked pyrazolylpyridine is of a 3-ferrocenyl derivative **8**.[7] It shows significant differences from those of **2** and bpy: the inter-ring bond is shorter, the N1′–N2′ bond in **8** is longer than the corresponding C–N bonds in **2** or bpy, the bite angle is smaller, and the N1···N2′ distance is narrower than in **2** (but about the same as in bpy). Still, the ideal binding distances (M–N) calculated for **8** are similar to those calculated for **2**. As expected, the sharper C2′–C2–N1 angle in bpy[15] leads to a smaller imine-to-imine (N1···N1′) span and a larger bite angle at closer range (M–N) than in either of the pyrazolylpyridines. Although there are three crystallographically distinct phen units in the crystal,[28] it is evident that the N–C–C–N moiety in phen is pulled slightly open, relative to that in bpy, by its C5–C6 linkage.

The STO-3G structure of *syn*-**4** resembled **1** while that of *anti*-**4** was more akin to **2**. Thus, the larger bite angle at closer range in the *syn* compound **1** can be ascribed to steric repulsions between H3 and the C4′ hydrogens, as suggested above by the H3···H4′ approaches, and not to intramolecular H-bonding.

Complexed Ligand Structures

Complexation here is accompanied by changes in virtually all bond lengths and angles, some of which must be due to inter-ligand or intermolecular crowding as well as to uncertainties in atomic positional parameters. The bond length changes are varied in size and sign and are without discernible

pattern. One can nevertheless discern some differences between the effects of complexation on our ligands and those on the *N'*,2-linked ligands or on bpy by comparison of the structures of complexes reported in the literature with reference to the free ligands **2**, **8**[7] and bpy.[15]

Our Zn and Ru complexes can be compared to the bpy complexes $[Ru(bpy)_3](PF_6)_2$,[29] $[Zn(bpy)_3](ClO_4)_2$[30] and $[Zn(bpy)_2(OH_2)](ClO_4)_2$.[21] One can also qualitatively compare our complexes with the reported structures of complexed *N'*,2-linked pyrazolylpyridines, i.e. $[Fe^{II}(\mathbf{6})_3](ClO_4)_2$[9] in both high- and low-spin forms, $[Ni^{II}(\mathbf{6})_3](ClO_4)_2$,[9] $Co^{II}(\mathbf{7})(OH_2)Cl_2$,[10] and the series[11] $[Cu^{I}(\mathbf{9})_2]BF_4$, $[Cu^{II}(\mathbf{9})_2](BF_4)_2$, $[Cu^{II}(\mathbf{9})$(tris(3-phenylpyrazol-1-yl) borate)]BF_4, and $[Cu^{II}(\mathbf{9})$(tris(3-(tetrahydrofuran-2-yl)pyrazol-1-yl)borate)]-BF_4. Beyond the Zn and Ru complexes discussed herein, there are three reported structures of complexes of other *C'*,2-linked pyrazolylpyridines, $Mo^0(\mathbf{10})(CO)_4$[12] and $Mo^{VI}(=O)(L)(O_2)_2$ (L=**11**[13] or **12**[14]), which can also be compared with the bpy analog $Mo^{VI}(=O)(bpy)(O_2)_2$.[31] The measurements used for comparison were obtained as described in the Experimental section. The notable points arising therefrom are summarized as follows:

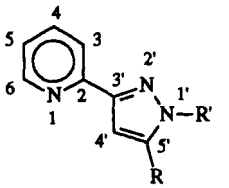

10 R = $C_5H_4FeC_5H_5$, R' = $CH_2COOCH_2CH_3$
11 R = H, R' = $CH_2COOCH_2CH_3$
12 R = H, R' = $CH_2CH_2CH_3$

(1) Upon complexation, **2** and **3** undergo some pinching of the C3'–C2–N1 angle at the pyridine end (about as much as is found in complexed bpy), but much more pinching of the corresponding angle at the pyrazole end (C2–C3'–N2'). For instance, one unit of **2** in $[Ru(\mathbf{2})_2(bpy)]^{2+}$ is pinched by 14.2° at the pyrazole junction, but only by 4.9° at the pyridine end, essentially the same value as in $Ru(bpy)_3^{2+}$ (4.8°). In contrast, complexation of *N'*,2-linked varieties **6**, **7** and **9** induces a more modest pinching at pyrazole (0.5°–9.5°) and variable pinching at pyridine (–1.2° to 6.3°). By way of comparison, the rigidity of phen precludes much angular variation in $Zn(phen)Cl_2$ (–0.7° and 1.5°).

(2) The metal centers are bound at much shorter distances than would be ideal (Table I) and such pinching serves to compensate for this. But it is

largely insufficient, such that the N–M bond vectors are slanted inwards from the ring bisectors. In one unit of **2** in $[Ru(\mathbf{2})_2(bpy)]^{2+}$, for example, the slant at pyrazole N is 20.8° whereas it is only 8.8° at pyridine N, a value akin to those in $Ru(bpy)_3^{2+}$ (10.1°) and in the Zn^{II} bpy complexes (6.2°–12.3°). In the complexes of the *N'*,2-linked pyrazolylpyridines, however, the slant is very pronounced, ranging from 21.1° to 38.5° at pyrazole N vs. a 10.2°–18.2° range at pyridine N. This can be directly attributed to the shorter bonds in the core N–N–C–N fragment.

(3) The M–N bonds at pyrazole N are consistently shorter than the bonds at pyridine N in all instances of complexed **2**, **3**, **6** and **7**, and this is consistent with the pattern in complexes of other azolylpyridines.[9,10,23] But this is true for the *N'*,2-linked **9** in only one complex, $[Cu^{II}(\mathbf{9})_2](BF_4)_2$. Admittedly, the other Cu complexes involve either distorted tetrahedral binding or strong inter-ligand crowding by the tris-(pyrazolyl)borates.

(4) At least in the Zn and Ru complexes, the M–N bonds to the pyridine portion of **2** or **3** are of similar length to those in bpy complexes. The shorter bonds to pyrazole N would therefore appear to indicate innately stronger binding to pyrazole N than to pyridine N. In general, this is purchased at a cost of stronger distortion of the pyrazole ring in the *C'*,2-linked materials, whereas both rings get distorted in the *N'*,2-linked varieties. Measurements of the average change in bond lengths show that the *C'*,2-linked varieties undergo more bond length distortions within the pyrazole rings than within the pyridine rings, whereas the opposite is true in most instances of complexed *N'*,2-linked pyrazolylpyridines.

(5) In most instances of complexed *N'*,2-linked pyrazolylpyridines there is a significant loss of ligand planarity, with either inter-ring twisting (0.1°–10.9°), especially strong with the C5'-methylated ligands **6** and **7** (8.0°–10.9°), or bowing (1.4°–15.9°) or both. These planar distortions most often lead to the metal lying significantly off the heterocyclic planes (by up to 40.0 pm). Another example is a 4.2° inter-ring twist in the Hg^{II} complex of **5**.[8] This twisting also occurs in the bpy complexes, with twists of up to 17.3° in $Zn(bpy)_3^{2+}$, except for one bpy unit in $[Zn(bpy)_2(OH_2)]^{2+}$ which remains flat but which undergoes relatively large bond length distortions to increase its bite angle. Walsh *et al.*[18] additionally report a dihedral angle of 12.9° between pyridine rings in $[Zn(bpy)_2(ONO)]NO_3$ and Herrman *et al.*[32] report four examples of similarly twisted bpy ligands in Mo^0 complexes. In contrast, the

C',2-linked varieties **2** and **3** retain their planarity in spite of the substitution at C4'. This is also true of **1**, which can be regarded as an internal H^+ complex. Ironically, only the Mo complexes of the C4'-unsubstituted **10** and **12**, with their poorly bound pyrazole rings at longer bond lengths, lose their planarity (see below).

(6) There is little kinship between the Mo complexes of **10**–**12** and the Zn and Ru complexes of **2** and **3**, and this is not due to the presence or absence of substitution at the pyrazole C4. Given the longer Mo–N bonds, one would expect smaller distortions of **10**–**12**. In fact, they suffer a similar amount of pinching at pyridine as in the Zn and Ru complexes (2.5°–5.8°) much as does the asymmetrically bound bpy in $Mo^{VI}(=O)(bpy)(O_2)_2$ (1.9° and 3.7°), but much more modest pinching at the pyrazoles (5.4°–6.5°). More significantly, the binding favors the pyridine rings rather than the pyrazoles, for the slanting of the M–N vector at pyridine is nearly nil (0.4°) in the two $Mo^{VI}(=O)(L)(O_2)_2$ complexes (L = **11** or **12**) but fairly pronounced at the pyrazoles (22.2° and 24.1°). Further and contrary to the usual finding, the Mo–N bonds are shorter to the pyridine than to the pyrazole. Similarly, the binding to one pyridine in $Mo^{VI}(=O)(bpy)(O_2)_2$ is much less slanted (–0.3°) with a shorter bond than it is to the other (5.1°). The binding asymmetry is attributable to a *trans* effect exerted by an oxo ligand,[31] and the oxo ligands in the complexes of **11** and **12** seem to favor pyridine over pyrazole. Mo^0(**10**)$(CO)_4$ shows more equally shared binding but still favors the pyridine (6.6°) over the pyrazole (17.1°). Further evidence of this preference is the degree to which the metal centers lie in the planes of the heterocycles. In the complexes of **10** and **12**, there is a significant inter-ring twist (6.4° and 6.6°), unlike with **2** and **3**, and the Mo centers lie closer to the pyridine planes (10.6 and 14.1 pm) than to the pyrazole planes (24.3 and 52.9 pm). Ligand **10** is additionally bowed by 4.7° better accommodate the metal at both sites.

Together, the modeling and crystallographic results suggest that the existence of **6** or **7** in flat, *syn* conformers is doubtful. Poorer π delocalization and poorer d–π overlap in the complexes can be anticipated. This may be at the source of the photochemical lability of $Ru(\mathbf{6})_3^{2+}$.[6a] This may also contribute to the higher-energy π^* orbitals and MLCT transitions generally observed in Ru^{II} complexes of *N'*,2-linked pyrazolylpyridines, but $Ru(\mathbf{5})_3^{2+}$, lacking the strong steric impediment of **6**, exhibits essentially the same electrochemical and electronic spectroscopic properties as $Ru(\mathbf{6})_3^{2+}$.[33]

Beyond impeding coplanarity, the proximity of the pyridine C3–H and the pyrazole C5′–CH_3 or C5′–H in complexes of *N′*,2-linked pyrazolylpyridines could also induce strong mutual shielding interactions in their NMR spectra. In contrast to ^{1}H-NMR signals, ^{13}C-NMR signals are less subject to through-space and ring currrent anisotropic effects originating in other ligands, yet, as a possible indication of the inter-ring proximity, the ^{13}C-NMR signals of such complexes[6,34] differ from those of bpy[6a] or of the *C′*,2-linked varieties[6b,25] in that one pyridine signal (C2 or C3) migrates *upfield* upon complexation, whereas every other signal with these ligands and every signal with the other ligands is shifted downfield.

Acknowledgements

The authors are grateful to Prof. D.V. Stynes and Mr. Isak Vernik for invaluable assistance in acquiring the structures reported here, to Dr. M.A. Halcrow for graciously communicating structural details for **8** and the Cu complexes in advance of publication, and to the Natural Sciences and Engineering Research Council for continued funding.

References

[1] E.C. Constable and P.J. Steel, *Coord. Chem. Rev.*, **93**, 205 (1989).
[2] Y. Luo and P.G. Potvin, *J. Org. Chem.*, **59**, 1761 (1994).
[3] P. Van der Valk and P.G. Potvin, *J. Org. Chem.*, **59**, 1766 (1994).
[4] R. Dash and P.G. Potvin, *Can. J. Chem.*, **70**, 2249 (1992).
[5] (a) D.L. Jameson and K.A. Goldsby, *J. Org. Chem.*, **55**, 4992 (1990); (b) D.L. Jameson, J.K. Blaho, K.T. Kruger and K.A. Goldsby, *Inorg. Chem.*, **28**, 4312 (1989); (c) A.J. Downard, G.E. Honey and P.J. Steel, *Inorg. Chem.*, **30**, 3733 (1991); (d) H. Brunner and T. Scheck, *Chem. Ber.*, **125**, 701 (1992).
[6] (a) P.J. Steel, F. Lahousse, D. Lerner and C. Marzin, *Inorg. Chem.*, **22**, 1488 (1983); (b) C. Marzin, F. Budde, P.J. Steel and D. Lerner, *New J. Chem.*, **11**, 33 (1987).
[7] R.J. Less, J.L.M. Wicks, N.P. Chatterton, M.J. Dewey, N.L. Cromhout, M.A. Halcrow and J.E. Davies, *J. Chem. Soc., Dalton Trans.*, 4055 (1996).
[8] A.J. Canty, C.V. Lee, N. Chaichit and B.M. Gatehouse, *Acta Crystallogr., Sect. B*, **38**, 743 (1982).
[9] A.T. Baker, N.J. Ferguson, H.A.Goodwin and A.D. Rae, *Aust. J. Chem.*, **42**, 623 (1989).
[10] A.T. Baker, N.J. Ferguson and H.A. Goodwin, *Aust. J. Chem.*, **37**, 2421 (1984).
[11] M.A. Halcrow, J.E. Davies, I.J. Scowen, H.R. Powell and P.R. Raithby (unpublished work).
[12] W.R. Thiel, T. Priermeier, D.A. Fiedler, A.M. Bond and M.R. Mattner, *J. Organometal. Chem.*, **514**, 137 (1996).
[13] W.R. Thiel, M. Angstl and T. Priermeier, *Chem. Ber.*, **127**, 2373 (1994).
[14] W.R. Thiel and T. Priermeier, *Angew. Chem., Intl. Ed. Engl.*, **34**, 1737 (1995).
[15] L.L. Merritt and E.D. Schroder, *Acta Crystallogr.*, **9**, 801 (1956).
[16] R.P. Thummel and Y. Jahng, *J. Org. Chem.*, **50**, 2407 (1985); C.A. Bessel, R.F. See, D.L. Jameson, M.R. Churchill and K.J. Takeuchi, *J. Chem. Soc., Dalton Trans.*, 3223 (1992).

[17] W.C. Hamilton, *Statistics in Physical Science* (Ronald Press, New York, 1964) pp. 157–162.
[18] A. Walsh, B. Walsh, B. Murphy and B.J. Hathaway, *Acta Crystallogr., Sect. B*, **37**, 1512 (1981).
[19] A.G. Orpen, L. Brammer, F.H. Allen, O. Kennard, D.G. Watson and R. Taylor, *J. Chem. Soc., Dalton Trans.*, S1 (1989).
[20] P.N.W. Baxter, J.A. Connor, W.B. Schweizer and J.D. Wallis, *J. Chem. Soc., Dalton Trans.*, 3015 (1992).
[21] M. Liu and S.K. Arora, *Acta Crystallogr., Sect. C*, **49**, 372 (1993).
[22] R. Alsfasser and H. Vahrenkamp, *Chem. Ber.*, **126**, 695 (1993); R. Alsfasser, M. Ruf, S. Trofimenko and H. Vahrenkamp, *Chem. Ber.*, **126**, 703 (1993).
[23] A.T. Baker, H.A. Goodwin and A.D. Rae, *Aust. J. Chem.*, **37**, 2431 (1984); *Inorg. Chem.*, **26**, 3513 (1987).
[24] C.W. Reimann, S. Block and A. Perloff, *Inorg. Chem.*, **5**, 1185 (1966).
[25] Y. Luo, P.C. Potvin, Y.-H. Tse and A.B.P. Lever, *Inorg. Chem.*, **35**, 5445 (1996).
[26] G. Tarrago, A. Ramdani, J. Elguero and M. Espada, *J. Heterocycl. Chem.*, **17**, 137 (1980).
[27] Y. Luo, Ph.D. Dissertation, York University, North York, Ontario, Canada, 1995.
[28] S. Nishigaki, H. Yoshioka and K. Nakatsu, *Acta Crystallogr., Sect. B*, **34**, 875 (1978).
[29] D.P. Rillema, D.S. Jones and H.A. Levy, *J. Chem. Soc., Chem. Commun.*, 849 (1979).
[30] X.-M. Chen, R.-Q. Wang and X.-L. Yu, *Acta Crystallogr., Sect. C*, **51**, 1545 (1995).
[31] E.O. Schlemper, G.N. Schrauzer and L.A. Hughes, *Polyhedron*, **3**, 377 (1984).
[32] W.A. Herrman, W.R. Thiel, J. Kuchler, J. Behm and E. Herdtweck, *Chem. Ber.*, **123**, 1963 (1990).
[33] P.J. Steel and E.C. Constable, *J. Chem. Soc., Dalton Trans.*, 1389 (1990).
[34] R. Hage, R. Prins, J.G. Haasnoot, J. Reedijk and J.G. Vos, *J. Chem. Soc., Dalton Trans.*, 1389 (1987).
[35] G.M. Sheldrick, *SHELXL-93, Program for Crystal Structure Determinations* (University of Göttingen, 1993).